

A DISTRIBUTED DESIGN ENVIRONMENT FOR ROTORCRAFT

P. Weiand, DLR Institute of Flight Systems, 38108 Braunschweig, Germany
M. Schmid, DLR Institute of Aerodynamics and Flow Technology, 38108 Braunschweig, Germany
M. Buchwald, Institute of Flight Systems, 38108 Braunschweig, Germany
D. Schwinn, Institute of Structures and Design, 70569 Stuttgart, Germany

Abstract

The German Aerospace Center (DLR) is currently developing a new environment for integrated rotorcraft design. This paper describes the fundamental features and approaches to generate the related design processes. The lessons learned from the DLR activities on fixed-wing design lead to the usage of distributed computation and the implantation of the CPACS data model adapted and extended for rotorcraft design. These activities are a DLR internal cooperation of the Institute of Flight Systems, the Institute of Aerodynamics and Flow Technology, and the Institute of Structures and Design. The tools implemented cover the conceptual and partly the preliminary design phase. Here the disciplines of sizing approaches, geometry generation, aerodynamic properties, mass estimation, and flight performance are considered. A quick design study is performed for a helicopter with typical HEMS (Helicopter Emergency Medical Service) capabilities.

Keywords

Rotorcraft design; distributed computing; integrated design; virtual configuration

NOTATIONS

Symbols

A_{MR}	Main rotor disc area, m ²
$C_l; C_m; C_n$	Moment coefficients around x, y and z axis, -
$C_{l\alpha}$	Lift slope of an airfoil section, -
C_T	Thrust coefficient, -
$C_x; C_y; C_z$	Force coefficients in x; y and z direction, -
c_{MR}	Main rotor blade mean chord length, m
G_{MTOM}	Weight force at maximum take-off mass, N
g	Gravitational acceleration, m/s ²
J_β	Flapping moment of inertia, kg m ²
l_{FUS}	Fuselage length, m
m_{BEM}	Basic empty mass, kg
m_{EQU}	Equipment mass, kg
m_F	Fuel mass, kg
m_{MTOM}	Maximum take-off mass, kg
m_{OM}	Operator mass, kg
m_P	Payload mass, kg
m_{SMM}	Specific mission mass, kg
$N_{bl,MR}$	Number of blades per main rotor, -
R_{MR}	Main rotor blade radius, m
R_{TR}	Tail rotor blade radius, m
T_{MR}	Main rotor thrust force, N
V_{cabin}	Cabin volume
$V_{tip,MR}$	Main rotor tip speed, m/s
γ_{MR}	Lock number of the main rotor blades, -
ρ	Air density, kg/m ³

σ_{MR}	Rotor density of main rotor, -
σ_{TR}	Rotor density of tail rotor, -
Ω_{MR}	Angular speed of main rotor, rad/sec

Abbreviations

ACT/FHS	Advanced Control Technology / Flying Helicopter Simulator
AFDD	U.S. Army Aeroflightdynamics Directorate
CPACS	Common Parametric Aircraft Configuration Schema
DLR	Deutsches Zentrum für Luft- und Raumfahrt (German Aerospace Center)
IRIS	Integrated Rotorcraft Initial Sizing
HEMS	Helicopter Emergency Medical Service
HOST	Helicopter Overall Simulation Tool
MDO	Multidisciplinary Design and Optimization
NDARC	NASA Design and Analysis of Rotorcraft
ONERA	Office national d'études et de recherches aérospatiales (The French Aerospace Lab)
RCE	Remote Component Environment
TLAR	Top Level Aircraft Requirements
TRIAD	Technologies for Rotorcraft in Integrated and Advanced Design

1 INTRODUCTION

1.1 Motivation

The central question to answer in every aerial vehicle design process is: "How large and how heavy should the new aircraft be in order to meet with the mission requirements?" An answer about how large an aircraft should be leads to the question about its take-off mass. The answer to its take-off mass leads consequently to the question how large do the aircraft's lift producing components need to be to carry its mass. This is a highly iterative and multidisciplinary task. In comparison to fixed-wing aircraft design, the design of rotorcraft is even more challenging. Because of the rotorcraft ability to vertically

take-off, hover and land, the choice of parameters to complete the sizing task is much more sensitive. In spite of its complex design the rotorcraft became a reliable transport vehicle for fast access to remote areas, especially for medical assistance and support. The ongoing motivation to extend its flight envelope or to increase its performance by integrating new technologies and to find new configurations require a very sophisticated development of the different computational tools considering their required input data, calculation time, robustness, and uncertainties.

1.2 Rotorcraft integrated design in the last years

In the last decade several research institutions conducted individual development on the field of integrated rotorcraft design. In 2009 Johnson [1] presented the NDARC (NASA Design and Analysis of Rotorcraft) code which is by now the state of the art rotorcraft design tool for US governmental investigations and university research. Example of the integration of NDARC into the overall design is presented by Sinsay [2]. On the European side Basset [3] presented the CREATION toolbox by ONERA (The French Aerospace Lab) focusing on the flight mechanic assessment on different levels of fidelity. The DLR carried out two projects in order to gain knowledge about setting up design processes for rotorcraft and, in the next step, extending the design process to new configurations, see Weiland [4]. These activities involved the DLR Institute of Flight Systems, the Institute of Aerodynamics and Flow Technology, and the Institute of Structures and Design. In 2018 DLR started the project TRIAD (Technologies for Rotorcraft in Integrated and Advanced Design) focusing on the integration of new technologies into different configurations in order to examine the influence on the overall design. Here the tools from the preceding projects will be adapted, extended and ported into the new design environment IRIS (Integrated Rotorcraft Initial Sizing). The first results of this new environment are presented in this paper.

1.3 Design theory

In the common literature the classical design process is divided into the three phases of the conceptual design, followed by the preliminary design, and finally the detailed design. FIG 1 outlines the design phases with the usual wording used for instance by Raymer [5] or Nicolai [6]. Here the conceptual design delivers the external configuration of the vehicle determining its dimensions. The preliminary design delivers the internal configuration including component arrangement and the full description of the external shape. The detailed design is the most comprehensive phase. It includes the complete production drawings, ground testing, prototypes, etc. In some references these three phases are extended to five by a trend study at the beginning and a proposal status between the preliminary and detailed design phase, see Layton [7]. If these phases are not mentioned explicitly the trend study is conducted at the beginning of the conceptual design and the proposal status comes at the end of the preliminary design phase. The trend study gives first ideas about the economic sense of a new project and marks the first decision whether to start a project or to focus on a different one. The proposal is the last point to consider executing the project. Due to the complexity of

the detailed design, there is no reasonable plan of terminating a project in the detailed design phase. Even though the small number of personnel working in the first phase compared to the second and in the second compared to the third, the results of the conceptual design already determine 65% of the life cycle costs of an aerial vehicle. By completing the preliminary design the grade of definition reaches 85% of the life cycle costs, see Roskam [8]. In traditional design approaches the design is frozen after completing each phase. New computational design methods featuring strongly networked tools allow switching between the first two phases. The working area of IRIS is the conceptual and partly the preliminary design with the ability to link the two design phases. Similar to the DLR design research on fixed-wing aircraft the features of a distributed computation and a universal data model for harmonization and exchange are considered.

Phase	Results	Grade of definition
Conceptual Design	geometry basic 3-side view	65%
	mass and balance centre of gravity component masses	
	flight performance drag levels & performance	
	cost factors & benefits	
Preliminary Design	basic internal arrangement component positions and volume demand	85%
	complete external configuration airfoil and blade twist local flow problems solved	
	major loads, stresses & deflections load cases are solved	
Detailed Design	detail design mechanisms joints, fittings & attachments damage assessment	100%
	prototype flight tests	
	design refinements as result of tests & operation	

FIG 1 Phases of design

2 DESIGN ENVIRONMENT

2.1 Tool classification

The tools available differ from each other by different levels of accuracy, required input, robustness and computational time. The objective of a design process is to find a suitable arrangement of the tools in order to increase the amount of information with every step or loop and decrease the uncertainties. Therefore the tools were divided into four groups, see FIG 2. To evaluate individual tools the amount of input, output and the physical method have to be considered. One important characteristic is the ability to perform quick and iterative computations in a sizing loop.

Level 0 tools use statistical and simple physical models. The computation is very fast. No loops are performed on this level. These tools mark the first dataset based on the TLARs (Top Level Aircraft Requirements) and on knowledge based data.

Level 1 tools conduct the primary sizing. This procedure typically iterates the maximum take-off mass. The tools use physical models of low to average complexity to achieve short computation time and hands-off calculation.

Level 2 tools are characterized by a more sophisticated physical modeling. Their pre- and post-processing procedures can still be performed automatically, but the required computation time exceeds the boundaries of iterative sizing. Considering the diminished robustness of the tools, the possibility to check the meaningfulness has to be given.

Level 3 tools have the highest fidelity and the most complex modeling. Pre- and post-processing procedures need additional input to solve necessary meshing tasks. In order to conduct full MDO (multidisciplinary design and optimization), secondary data has to be stored. The computation time is the highest. No level 3 tools are integrated into the presented design environment.

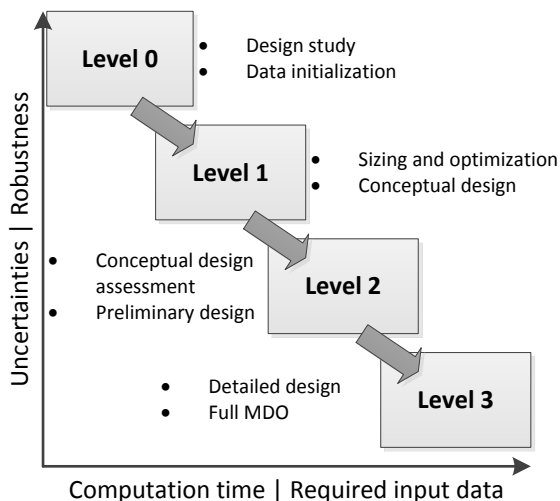


FIG 2 Classification of tools

2.2 Process architecture

According to the characteristics of the tool classification, the design process including level 0 to level 2 tools is arranged in three main sections, see FIG 3. The initialization is the first main section. Here the initial data set is computed by the level 0 tools. The second main section is the primary sizing. It is divided into a design section and an analysis section. The design section performs the sizing of the external configuration. The analysis section performs the recalculation of the initial mass fractions. Here a flight performance calculation delivering the required fuel mass and basic empty mass is computed by determining and summing up the individual component masses. The amount of data computed in the sizing loop must be sufficient to create a flight mechanic

simulation model. The recalculation of the mass fractions delivers the updated maximum take-off mass and the new input for the next iteration. The convergence of the masses and external configuration derives a consistent design, which brings the mass of the vehicle, its outer dimensions and the required flight / transport performance into a sensible correlation. After sizing, the assessment and the higher fidelity computation are performed in the third main section with the level 2 tools. This may include a series of flight simulations in order to compute load cases for a finite element structural analysis (see Schwinn [9]). The results of these tools can be used to update the technology factors for the conceptual sizing loop. Changes and adaption of the design can be made. An updated data set with the need for resizing is led back to the primary sizing loop.

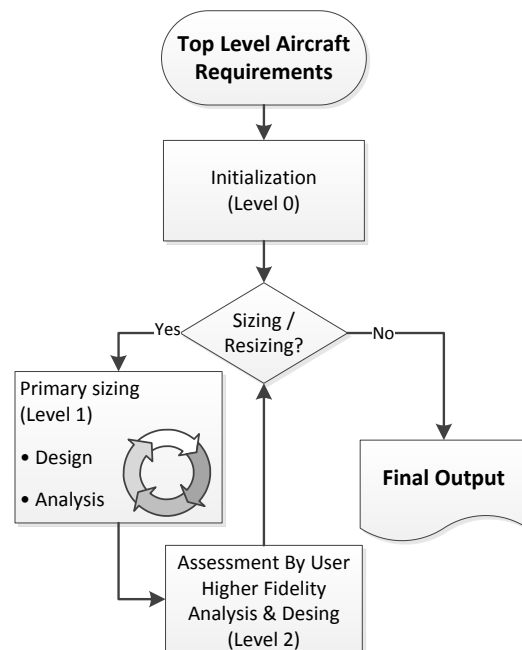


FIG 3 Flowchart of the main functions of the design environment

2.3 Implementation of flight simulation tool

As mentioned above the ability to perform flight mechanic simulations inside the primary sizing loop determines the amount of data which has to be computed by the initialization main section and the design section. For the flight simulation and performance calculation in this design environment HOST (Helicopter Overall Simulation Tool) is used. HOST was originally designed by Airbus Helicopters (at that time Eurocopter) in the 1990s, see Benoit [10]. Its three main functions are trim calculations, time domain simulations and the calculation of linear equivalent systems.

As part of the level 1 tools the trim function is used to conduct the flight performance calculation. The flight performance calculation is part of the fuel estimation loop and is carried out in batch mode. Within this tool the pre- and post-processing procedures have to work automatically. Different shell and Python scripts are used

for pre- and post-processing and for the generation of a flight mechanical model. After the calculation of the trim points the results are extracted from the simulation environment and stored in the design environment.

2.4 Collaboration and network

The features described above require a very sophisticated networking between the different computational tools which were usually hosted by individual specialists. Following the good experiences of DLR's fixed-wing design summarized by Liersch [11], the approach of a distributed computation was also followed right from the beginning. The network connection of the tools is ensured by the DLR developed collaboration software RCE (Remote Component Environment), see Bachmann [12] and Seider [13]. RCE is an open source software and the common resource for distributed processes in DLR projects. Tools can be stored on different servers and made available to design teams. The tools can be arranged in a graphical user interface.

The second important resource is a uniform data model to ensure the communication between the tools. The CPACS (Common Parametric Aircraft Configuration Schema) data model, see Böhnke [14] and Nagel [15], was originally developed as a communication language for fixed-wing design. CPACS has a strongly hierarchical XML structure and serves as a universal language for all integrated tools. The stored data include geometry, performance, requirements, component masses and more. The combination of CPACS and RCE has shown to be reliable (see Liersch [11]). Following the good experience with fixed-wing design CPACS was extended for rotorcraft design and implemented into the present rotorcraft design environment. The parametric description of fuselage, wings and stabilizers does not differ between the two types of aircraft. The description of the rotors, the mass breakdown, and flight performance requires some extensions. The further development of CPACS is an ongoing process for both fixed- and rotary-wing applications.

Since every tool uses the same CPACS data model for input and output, the process can easily be arranged. Adding and rearranging tools becomes an easy task of drag and drop and wiring the tools.

3 INITIALIZATION OF FIRST DATA

3.1 Requirements and configuration

Generating the first data requires reading the requirements and producing the first configuration out of it. These computations are very simple and straightforward. The tools used here are assigned to level 0. The requirements usually are divided into three groups.

- The technical requirements determine the boundaries and demands for the external configuration. They describe and, if necessary, extrapolate the state of the art related to the specific design.

- The mission requirements give information about the use of the rotorcraft, which is at minimum the triplet of range, payload and flight speed.
- The performance requirements describe the flight conditions of the design mission profile and describe the flight envelope.

Several approaches were conducted to find the minimum required TLARs for which the design process can be expected to produce reasonable outputs. This led to the question how much information could be derived from statistical regressions and knowledge based parametrization and what was the fuzziness of the configuration with respect to the intended use of the rotorcraft. Five parameters listed in TAB 1 have been found to be the minimum TLARs to initialize the process. The first three parameters are the triplet of the most simple flight performance. They determine how much mass shall be transported over what distance at which desired airspeed. The next two parameters determine the rotorcraft configuration. Besides the main rotor arrangement, specifying the number of main rotor blades has been found to be sensible. Additional requirements can be added in order to specify the results more clearly. This optional input may affect the sizing of the rotors with respect to a desired flight performance and the dimensions of the fuselage with respect to a required cabin layout. Sections 3.3, 3.4 and 4.2.1 will deal with this topic in more detail.

<i>Name</i>	<i>Type of parameter</i>	<i>Unit</i>
Specific mission mass	continuous	kg
cruise speed	continuous	m/s
range	continuous	m
number of main rotor blades	discrete	-
main rotor configuration	selection	-

TAB 1 Minimum TLARs to start the process

3.2 Mass fractions

The empirical equations introduced in the following subsections to describe e.g. the initial mass fractions or the rotor dimensions were derived from a statistical evaluation of 159 existing helicopter configurations.

The maximum take-off mass comprises the basic empty mass, the fuel mass and the specific mission mass given in equation (1). The specific mission mass, as the second part of the useable load besides the fuel, is the sum of the payload, the operators mass and the specific mission equipment mass, see equation (2). The result for equation (2) has to be defined by the requirements. Computing the fuel mass and basic empty mass to solve equation (1) is the fundamental task of the conceptual design.

$$(1) \quad m_{\text{MTOM}} = m_{\text{BEM}} + m_{\text{F}} + m_{\text{SMM}}$$

$$(2) \quad m_{\text{SMM}} = m_{\text{P}} + m_{\text{OM}} + m_{\text{EQU}}$$

Experience shows a good relation between the maximum take-off mass and the basic empty mass. The specific mission mass and the fuel mass form the useable mass. The true problem for initialization is that mission scenarios for rotorcraft are much more specific for each design than for fixed-wing. It is obvious that different ratios of specific mission mass and fuel mass are possible for one maximum take-off mass. This is the fundamental reason for iterative computations in a sizing loop. In order to start such a loop an initial configuration has to be derived. The estimation of m_{BEM} and m_F by equations (3) and (4) is one possibility, considering an increasing amount of equipment in equation (2) for configurations resulting in more than 5 t m_{MTOM} .

$$(3) \quad m_{BEM} = 2.9m_{SML}^{0.9275}$$

$$(4) \quad m_F = 4.8m_{SML}^{0.6925}$$

3.3 First dimensions of the rotors

The maximum take-off mass is the basis for the sizing of the external configuration. Most important are the dimensions of the main rotor or rotors. The thrust related to tip speed and disc area is given by equation (5). The rotor solidity describes the ratio blade area to the rotor disc area and is given by equation (6).

$$(5) \quad C_T = \frac{T_{MR}}{\rho v_{tip}^2 \pi R_{MR}^2}$$

$$(6) \quad \sigma = \frac{N_{bl} c_{MR}}{\pi R_{MR}}$$

The blade loading describes the thrust with regard to the blade area. It is derived by dividing equation (5) by equation (6) leading to equation (7). Values of more than 0.12 for the blade loading indicate first flow separations somewhere on the rotor disc (see van der Wall [16]).

$$(7) \quad \frac{C_T}{\sigma} = \frac{m_{MTOM} g}{\rho v_{tip}^2 N_{bl} c_{MR} R_{MR}}$$

Reasonable regression curves must meet with aerodynamic boundaries of rotors. Suitable dimensions for the main rotor are given by equations (8) and (9). For configurations with two main rotors a simple lift sharing can be applied adapting the input mass.

$$(8) \quad R_{MR} = 0.226m_{MTOM}^{0.392}$$

$$(9) \quad \sigma_{MR} = 0.012m_{MTOM}^{0.221}$$

FIG 4 shows the results of equations (7) to (9) for a single main rotor.

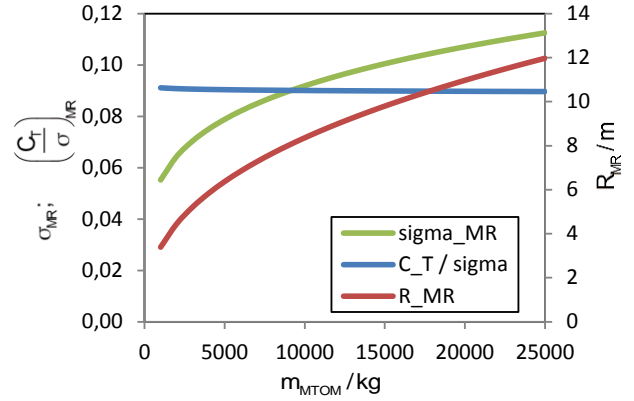


FIG 4 Properties of the main rotor with statistical sizing approach

Density equals ground conditions with 1.225 kg/m^3 and the tip speed was set to 210 m/s. The thrust corresponds to hover with m_{MTOM} . The graphs show rotor radius as well as solidity increasing with m_{MTOM} , but the gap is slightly closing. The resulting blade loading is slightly decreasing from 0.091 to 0.09 within reasonable values.

In addition to equations (8) and (9), the equations (10) and (11) define the radius and solidity of a tail rotor.

$$(10) \quad R_{TR} = 0.032m_{MTOM}^{0.438}$$

$$(11) \quad \sigma_{TR} = 0.018m_{MTOM}^{0.241}$$

3.4 Fuselage dimensions

With the evaluation of the TLARs a first sizing of the fuselage is performed in order to determine the dimensions of every fuselage part. The individual parts of the overall fuselage are shown in FIG 5. Basically the fuselage comprises the body, the engine cowling and the tail boom. The body is parted into "Fuselage Front", "Fuselage Mid" and "Fuselage Rear". The front consists of the cockpit, the avionics and optionally a retractable landing gear. The "Fuselage Mid" part holds the cabin volume. The "Fuselage Rear" part can have doors, a stern ramp or a cargo hold.

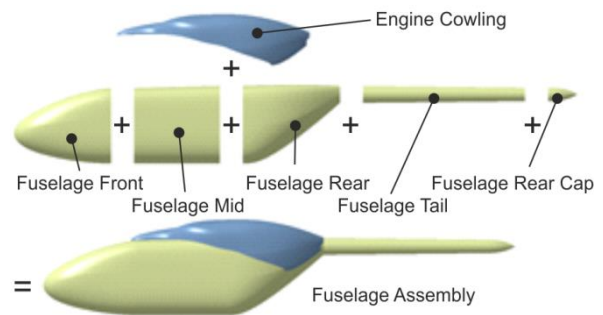


FIG 5 Parts of a generic fuselage model

If a tail boom is required, it consists of the "Fuselage Tail" and the "Fuselage Rear Cap". The sizing starts with the

cross section of the fuselage. The cross section has to consider the cabin dimensions plus additional space for structure, systems, and fuel tank. The lengths of the front and rear parts are related to the fuselage height. The length of the tail boom is defined by the position of the tail rotor and the stabilizers. The sizing of the body under the rotors can be statistical, but produces more reasonable results when additional inputs as shown in TAB 2 are taken into account.

Name	Type of parameter	Unit
cabin height	continuous	m
cabin width	continuous	m
cabin length	continuous	m
cargo hold payload fraction	continuous	-

TAB 2 Optional requirements for cabin and fuselage

In addition to height, width and length of the cabin the cargo hold payload fraction gives the share of the payload, which is stored in an optional cargo hold in the "Fuselage Rear" part according to FIG 5. Cargo hold payload fraction and cabin dimensions can be added independently. The parametrization of the fuselage parts is the basis for generating a 3D model inside the sizing loop (see section 4.2.2).

4 PRIMARY SIZING

4.1 Convergence of sizing loop

All subsequent level 1 tools are working iteratively. Here sizing, geometry generation, aerodynamics, flight performance, and mass estimation are run successively. A typical convergence criterion for the maximum take-off mass is 0.5 % relative deviation. Until convergence is reached the process works hands off, including the generation of the flight mechanical model and the performance calculation for the individual flight profile with HOST.

4.2 Sizing section

4.2.1 Rotor sizing

There are different modes for the sizing of the main rotor inside the primary loop which extend the level 0 sizing by using regression curves. Some of these modes can be combined with each other in order to meet with different sets of design parameters. The following features are covered for the sizing of the main rotor disc:

- Sizing with regression curves according to equations (8) and (9).
- Sizing with a specified disc loading
- Sizing with a specified blade loading in connection with different combinations of flight altitude and ambient temperature.
- Setting a boundary for a maximum allowed rotor radius.
- Setting a constant rotor radius and sizing the rotor solidity (constant blade loading with a variable disc loading)

A typical design approach explains the use of these modes. Assume a disc loading of 400 N/m^2 is given which may be the result from an assessment of the requirements and further optimization. Because of requirements for ship deck landing and hangars the maximum rotor radius is limited to 8 m. With respect to fast forward flight and maneuverability a suitable blade loading of 0.08 is chosen for hovering with m_{MTOM} at zero altitude ISA (International Standard Atmosphere), based on previous design experiences. FIG 6 shows the radius and solidity for m_{MTOM} from 6 t to 12 t. The single main rotor has five blades and a tip speed of 210 m/s.

With increasing take-off mass the rotor radius is increasing as well, keeping the disc loading constant. For constant thrust coefficient and a required blade loading the solidity is constant as well until the maximum radius of 8 m is reached. Now with increasing disc loading, the solidity has to be increased to meet with the blade loading requirement of 0.08. Here the aspect ratio of the blades decreases from 17.2 to 11.8.

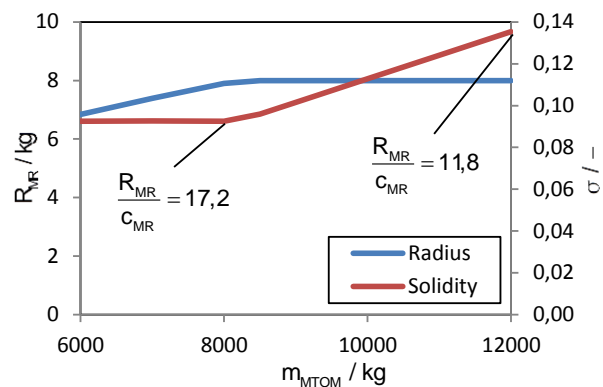


FIG 6 Rotor radius and solidity for a sizing example with 400 N/m^2 disc loading, a blade loading of 0.08 and maximum radius of 8 m for different m_{MTOM}

Beyond these analytical approaches, a knowledge-based optimization of the blade plan form as well as an optimization of the blade twist can be conducted (see Krenik [17]). An optional twist optimization minimizes the total power for a desired flight condition. A flight performance calculation requires the aerodynamic properties of the fuselage, hence the computation of the fuselage aerodynamics and the generation of the geometry have to be carried out in a previous step.

One important parameter of aeromechanic similarity is the Lock number γ_{MR} which describes the ratio of aerodynamic forces to gyroscopic forces of a rotor blade, as defined in equation (12). To meet with the properties of a specific rotor technology it is functional to choose the Lock number as a design parameter. Equation (12) is solved for the flapping moment of inertia. Calculating J_β from the design Lock number and the present blade dimensions yields reasonable input for the later trim and performance calculation.

$$(12) \quad \gamma_{MR} = \frac{\rho \cdot C_{L\alpha} \cdot c_{MR} \cdot R_{MR}^4}{J_{\beta}}$$

4.2.2 Geometry generation

In section 3.4 the initial sizing of the fuselage parts was described according to the fuselage assembly shown in FIG 5. A complex geometry generation by Kunze [18] is coupled with the commercial software CATIA V5, see FIG 7 for three examples. Different templates for every fuselage part are saved. The templates for every part can be modified to nearly any arbitrary shape in order to conduct scaling from existing configurations or completely new ones.

Generic fuselage templates are implemented for rotorcraft configurations with a tail boom such as the standard configuration with main/tail rotor arrangement or a coaxial rotor arrangement. Besides the tail boom configurations the positioning of two drive train cowlings for tandem rotors is implemented. The use of wings and propellers for compound configurations is possible too. The surface model, as the basis for aerodynamic and structural computations, is saved in the CPACS file.

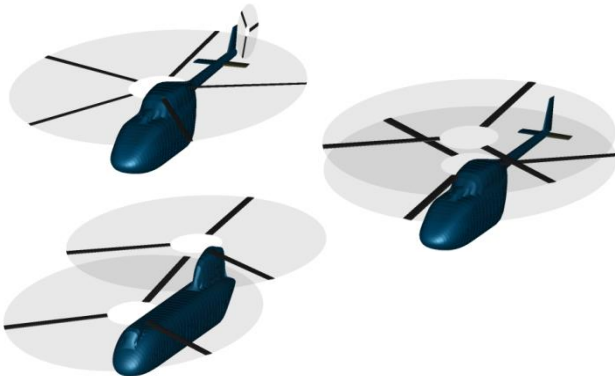


FIG 7 Three examples for rotorcraft configurations with different dimensions and from different templates (top left: main/tail rotor configuration; middle right: coaxial configuration; bottom left: tandem configuration)

4.2.3 Fuselage aerodynamics

As mentioned in section 2.3 HOST was implemented into the sizing loop to conduct the trim and performance calculations. To perform the complete trim an extended knowledge of the aerodynamic properties of the fuselage is essential. The algorithm inside HOST needs three force and three moment coefficients. The first option to compute the aerodynamic coefficients of the fuselage is by applying a panel method on the generated surface model described in section 4.2.2. In the present approach a linearized 3D panel method is harmonized with the CPACS data model, see Kunze [18]. This tool is based on the commercial calculation tool VSAERO, see Maskew [19]. The code applies potential flow theory by modelling inviscid and incompressible flow. If desired, compressibility corrections can be applied. To account for the viscous drag, the approach is extended by an integral boundary layer formulation. Within this calculation the transition and separation of the boundary layer can be estimated. FIG 8

shows the streamlines on the surface of a scalable 3D model. The streamlines are colored by the shape factor H , showing the estimated transition in the areas where the color changes from green to red. The streamlines end on the estimated separation line. Experience has shown that the prediction of the separation line gets coarser with increasing area of separation.

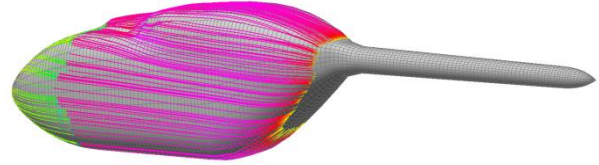


FIG 8 Streamlines on the surface of conventional fuselage model including transition forecast. The streamlines end on the separation line.

The results of this aerodynamic computation only take the clean surface of the fuselage into account. In order to cover further components like the rotor hub, landing gear, antennas or other attachments, a correction of the coefficients by handbook methods is required. The corresponding drag areas of the individual components are placed on the location of impact on the fuselage. An estimated drag area of the rotor hub was derived from the investigation presented by Keys [20].

The second possibility is to scale existing aerodynamic data by similarity laws. Equation (13) shows the approach for force and moment coefficients with the cabin volume as a reference.

$$(13) \quad \begin{pmatrix} C_x \\ C_y \\ C_z \\ C_l \\ C_m \\ C_n \end{pmatrix} = \begin{pmatrix} C_{x,ref} \\ C_{y,ref} \\ C_{z,ref} \\ C_{l,ref} \\ C_{m,ref} \\ C_{n,ref} \end{pmatrix} \left(\frac{V_{cabin}}{V_{cabin,ref}} \right)^{\frac{2}{3}}$$

By assuming the volume of the rotorcraft to be proportional to its mass, the scaling factor can also be written as the ratio of the maximum take-off masses, see equation (14).

$$(14) \quad \frac{V_{cabin}}{V_{cabin,ref}} \approx \frac{m_{MTOM}}{m_{MTOM,ref}}$$

This scaling approach is a very fast computation of the aerodynamic properties. It is an adaption of the dimensions of a known fuselage; hence for this approach a computation of the geometry is not required inside the primary sizing. Adding the geometry to the CPACS data model can be done after the sizing has converged.

4.3 Analysis Section

4.3.1 Fuel mass estimation

The fuel mass estimation consists of a small loop including the performance calculation, a script to update the fuel

mass, and a converger. After the generation of a HOST model from the CPACS data model including the trim and equilibrium law files the trim is calculated in batch mode for the flight segments of the mission profile. The required fuel is averaged between all trim points. The most simple mission profile consists of only one segment. Here the vehicle simply reaches a total distance without any reserve. Convergence is reached when the estimated range meets the required range and the relative fuel mass deviation is less than 1 %.

4.3.2 Component mass estimation

The computation of the basic empty mass is conducted by the summation of the component masses. The individual component masses can be estimated by four different methods. These methods have been published by Beltramo [21], Layton [7], Prouty [22] and the AFDD (U.S. Army Aeroflightdynamics Directorate) as presented by Johnson [1]. In addition, Palasis [23] presented a combination of Beltramo's and Layton's methods. It is possible to individually choose between the methods. However, the AFDD models are the most recently presented ones and require the highest number of input parameters among the implemented methods. For many component masses, the overall maximum take-off mass is one input parameter. Consequently the computation of the basic empty mass changes the overall mass which in turn requires its reevaluation. Therefore, the mass estimation is conducted in a nested loop to deliver a converged m_{BEM} for a given configuration. This was found to be very suitable for a better convergence of the primary loop iterating m_{MTOM} .

5 EVALUATION

5.1 A quick design study

The DLR has extensive experience with its research helicopter ACT/FHS (Advanced Control Technology / Flying Helicopter Simulator). This is a highly modified variant of an EC135, a typical option for HEMS operations below 3 t maximum take-off mass (see FIG 9 and Kaletka [24]). A validated HOST model for the ACT/FHS is available. Experience has shown that it is a good reference for a design study. TAB 3 shows the minimum TLARs identified by DLR for the ACT/FHS.

Parameter	Value
payload mass	809 kg
cruise speed	65 m/s
range	615 km
number of main rotor blades	4
main rotor configuration	standard

TAB 3 Minimum TLARs identified for the ACT/FHS research helicopter

The cabin volume was averaged to a cubic shape; reasonable requirements for the interior were derived and listed in TAB 4. Here only the room behind the two cockpit seats is considered.

cabin height	1.25 m
cabin width	1.5 m
cabin length	1.7 m
cargo hold payload fraction	0.2

TAB 4 Additional requirements for the cabin of an ACT/FHS like rotorcraft

Computation was started with the input from TAB 3 and TAB 4. Fuselage templates were chosen with a simplified shape of the ACT/FHS. FIG 9 compares the 3D external configuration of the ACT/FHS with the design output. For the present design study a three-bladed tail rotor was chosen, since the complete scalable model of a Fenestron including collector, rotor, stator and diffuser is not implemented at the moment.



FIG 9 Top: Reference configuration ACT/FHS Bottom: output 3D model from IRIS

The resulting dimensions of the configuration are listed in TAB 5. The parameters mainly show a good agreement. The most significant divergences are recognized between the basic empty mass and the fuel mass. Obviously these parameters are the main outputs of the conceptual sizing and therefore the sum of all uncertainties. Luckily for this case study these errors nearly cancel each other out.

The useable mass, i.e. the sum of fuel and specific mission mass, of the virtual configuration is 1333 kg and 2.42 % less the useable mass of the reference aircraft (1366 kg). In order to find reasonable trim masses for a comparison of the flight performance curves the ratio of the usable mass with respect to the flight mass was staggered into 20 %, 40 %, 60 %, 80 % and 100 % for both configurations. The sum of useable mass and basic empty mass resulted in slightly different flight masses as shown in FIG 10. The power required plotted in FIG 10 is the sum of the main rotor and the anti-torque power. Gear losses and systems power are not included in this graph. The solid lines represent the performance curves of the virtual configuration and the dashed lines represent the reference. Induced power and airfoil power are slightly higher for the virtual configuration. As seen in the labels of FIG 10 the flight masses of the virtual configuration are higher compared to the reference. The airfoils used for the sizing during the design study are NACA 23012 which

have a worse glide ratio and show an increased airfoil drag in comparison to the original airfoils developed by Airbus. On the other side the parasite drag of the virtual fuselage is a little bit lower because of the incomplete considered attachment on the surface. This results in bridging the gap between the two required power curves at higher flight speeds.

	ACT / FHS reference	IRIS virtual	deviation
m_{MTOM} , kg	2910	2985	2.58 %
m_{BEM} , kg	1544	1652	6.99 %
m_F , kg	557	524	-5.92 %
R_{MR} , m	5.1	5.2	1.90 %
C_{MR} , m	0.289	0.286	-1.04 %
l_{FUS} , m	10.21	9.92	-2.80 %
$\frac{G_{MTOM}}{A_{MR}}$, $\frac{N}{m^2}$	349	345	-1.22 %
Ω_{MR} , $\frac{rad}{sec}$	41.4	40.4	-2.29 %
σ , -	0.072	0.070	-2.68 %
$\frac{C_T}{\sigma}$, -	0.089	0.091	2.38 %

TAB 5 Characteristic parameters of the reference configuration and the case study

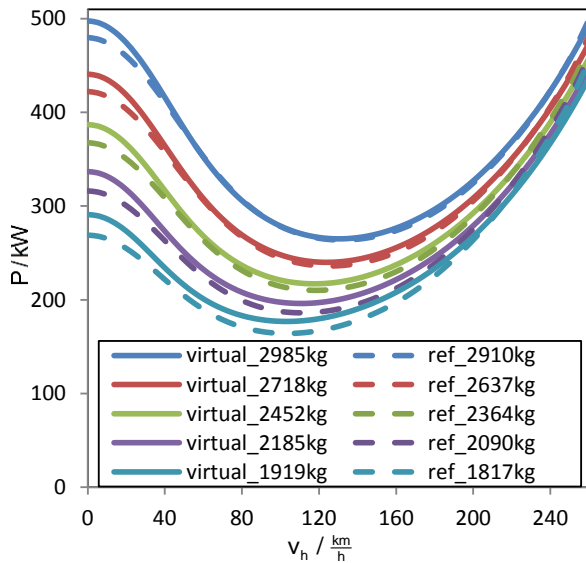


FIG 10 Flight performance curves from the ACT/FHS HOST model in comparison to the design output

A breakdown of the basic empty mass is given in TAB 6. The validation of the individual component masses is difficult because of the lack of access to reliable reference data. For instance the mass of the transmission listed in TAB 6 seems to be very low. However, summing up all components results in a basic empty mass 6.99 % higher than the reference.

Mass component	m_{comp} / kg
Rotor group	220
Engines	201
Transmission	23
Fuselage	266
Empennage	15
Landing gear	131
Nacelle	44
Air-condition & anti-icing	17
Auxiliary power	42
Avionics	133
Electrics	130
Fight controls	55
Fuel system	55
Furnishing	193
Hydraulics	15
Instruments	48
Load handling	65
Basic empty mass	$\Sigma =$ 1,652

TAB 6 Breakdown of the component masses for the virtual configuration

5.2 Variation of design parameters

The sensitivity of the tools is shown with a variation of the design parameters. Therefore a variation of the disc loading is conducted while keeping a constant blade loading. TAB 5 shows values for the disc loading from 345 to 349 N/m² and blade loadings from 0.089 to 0.091. A reasonable baseline shall be given with a disc loading of 350 N/m² and a blade loading of 0.09. The disc loading is now varied to four additional levels, two above and two beyond the baseline. The resulting mass contributions for 250 N/m² to 450 N/m² disc loading are shown in TAB 7.

$\frac{G_{MTOM}}{A_{MR}}$, $\frac{N}{m^2}$	250	300	350	400	450
m_{MTOM} / kg	3,029	2,999	2,988	2,987	2,996
m_{BEM} / kg	1,718	1,677	1,653	1,636	1,629
m_F / kg	502	513	526	541	558

TAB 7 Primary mass contributions for a variation of the disc loading

The maximum take-off mass has a minimum between 350 and 400 N/m². It can be shown how the basic empty mass decreases with increasing disc loading, while the fuel mass increases. FIG 11 shows the rotor radius and blade aspect ratio over the disc loading.

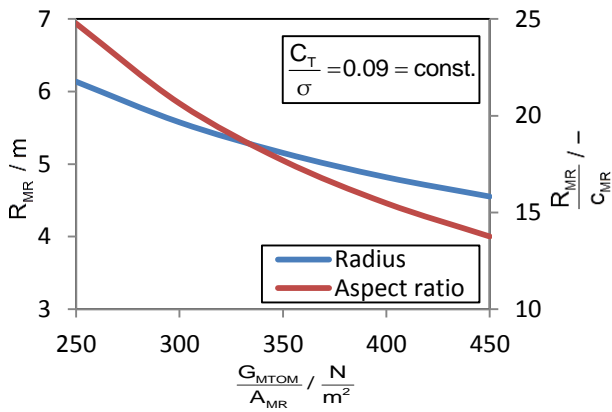


FIG 11 Rotor radius and aspect ratio over disc loading with constant blade loading

For the baseline the blade has a radius of 5.15 m with an aspect ratio of 15.5. By increasing the disc loading the aspect ratio decreases from 24.8 to 13.8 resulting in a significantly increased blade mass with disc loadings below 350 N/m². The fuel mass is computed for a single flight segment of 615 km at 65 m/s flight speed resulting in a low induced power for the design point. Considering a certain hover efficiency it seems a disc loading of more than 350 N/m² would lead to a strong increase of the required fuel mass at off-design flight conditions.

Another variation of design parameters is applied by including additional performance requirements for hot & high flight conditions. The most popular design criterion for hot and high operations is safe hovering out-of-ground effect at an altitude of 1830 m with a temperature of 35°C (the Army Hot Day: 6000 ft and 95°F). Experience has shown that rotorcraft should not be operated with a blade loading of more than 0.11 to ensure take-off, hover and safe control in case of potential disturbances.

The power available through the engines, due to one engine inoperative requirements, is considered to be sufficient. The mission requirements will not be effected. A comparison of the baseline configuration with the “hot & high” capable configuration is shown in TAB 8. The most recognizable deviation is the increased mean chord and rotor solidity. The blade loading for ground conditions with maximum take-off mass drops from 0.09 to 0.083. The resulting rise of airfoil power causes a rise of required fuel and a rise of the maximum take-off mass in connection with a higher basic empty mass.

	Baseline vehicle	Hot & high variation	deviation
m_{MTOM} , kg	2,988	3,061	2.43%
m_{BEM} , kg	1,653	1,705	3.14%
m_F , kg	526	547	3.96%
R_{MR} , m	5.15	5.22	1.20%
C_{MR} , m	0.291	0.322	10.51%
Ω_{MR} , $\frac{rad}{sec}$	40.7	40.3	-1.08%
σ_{MR} , -	0.072	0.079	9.20%
$\frac{C_T}{\sigma}$, -	0.090	0.083	-8.60%
$\frac{m_{SML}}{m_{MTOM}}$, -	0.27	0.26	-2.38%

TAB 8 Variation of the rotor design parameters for hot & high performance requirements

6 SUMMARY

This paper demonstrated a new setup for the DLR rotorcraft design environment. The fundamental features of IRIS are:

- Distributed computation on different servers.
- A direct implementation of a flight mechanic simulation tool into the sizing loop.
- Flexible setup of the tools for highly modular workflow characteristics.
- Usage of a universal data model for tool communication.

The level 1 sizing loop was used for a conceptual sizing study of a HEMS capable helicopter with about 3 t maximum take-off mass. The comparison to an existing reference helicopter showed good agreements with the ability for trade-off studies taking into account different sorts of requirements. The variation of design parameters demonstrated the impact of small changes on the overall design. The capability of tracking the influence of new technologies and optimization results through a complex configuration is achieved. The extension of sizing and trim algorithms to modern configurations with combined lift from rotating and fixed wings and an extended flight envelope will be the next challenge.

7 REFERENCES

1. Johnson, W.: NDARC - NASA Design and Analysis of Rotorcraft. NASA/TP-2009-215402. Ames Research Center, Moffett Field, CA, USA (2009)
2. Jeffrey D. Sinsay: Re-imagining Rotorcraft Advanced Design. Rotorcraft Virtual Engineering Conference, Liverpool, UK, 8 - 10 November, 2016
3. Basset, P.-M., Tremolet, A., Cuzieux, F., Reboul, G., Costes, M., Tristrant, D., Petot D.: C.R.E.A.T.I.O.N. the Onera Multi-Level Rotorcraft Concepts Evaluation Tool: The Foundations. Future Vertical Lift Aircraft Design Conference, San Francisco, CA, USA, 18 January 2012
4. Weiand, P., Schwinn, D., Schmid, M., Buchwald, M.: A Multidisciplinary Process for Integrated Rotorcraft Design. 43rd European Rotorcraft Forum, Milano, I, 12 -15 September, 2017
5. Raymer, D.P.: Aircraft design. A conceptual approach, 5th edn. AIAA education series. AIAA American Inst. of Aeronautics and Astronautics, Reston, Va. (2012)
6. Nicolai, L.M., Carichner, G.E.: Fundamentals of aircraft and airship design. AIAA education series. AIAA American Inst. of Aeronautics and Astronautics, Reston, Va. (2010)
7. Layton, D.M.: Introduction to Helicopter Design. AIAA Professional Studies Series, Salinas, CA, USA (1992)
8. Roskam, J.: Airplane cost estimation. Design, development, manufacturing and operating, 3rd edn. Airplane design, / Jan Roskam ; Part VIII. DARcorporation, Lawrence, Kan. (2006)
9. Schwinn, D., Weiand, P., Schmid, M.: Structural Analysis of a Rotorcraft Fuselage in a Multidisciplinary Environment. NAFEMS World, Stockholm, S, 11-14 June, 2017
10. Benoit, B., Dequin, A.-M., Kampa, K., Grünhagen, W. von, Basset, P.-M., Gimonet, B.: HOST, a General Helicopter Simulation Tool for Germany and France. American Helicopter Society 56th Annual Forum, Virginia Beach, Virginia, USA, 2 - 4 May, 2000
11. Liersch, C.M., Hepperle, M.: A distributed toolbox for multidisciplinary preliminary aircraft design. CEAS Aeronaut J (2011). doi: 10.1007/s13272-011-0024-6
12. Bachmann, A., Kunde, M., Litz, M., Schreiber, A.: Advances in Generalization and Decoupling of Software Parts in a Scientific Simulation Workflow System. 4th International Conference on Advanced Engineering Computing and Applications in Sciences - ADVCOMP 2010, Florence, Italy, 25-30 October, 2010
13. Seider, D., Fischer, P.M., Litz, M., Schreiber, A., Gerndt, A.: Open Source Software Framework for Applications in Aeronautics and Space, Big Sky, Montana,, 3 March 2012
14. Böhnke, D., Litz, M., Rudolph, S.: Evaluation of Modeling Languages for Preliminary Airplane Design in Multidisciplinary Design Environments. Deutscher Luft- und Raumfahrtkongress 2010, Hamburg, D, 31 August 2010
15. Nagel, B., Böhnke, D., Gollnick, V., Schmollgruber, P., Rizzi, A., La Rocca, G., Alonso, J.J.: Communication in Aircraft Design: Can we establish a common language? 28th International Congress of the Aeronautical Science, Brisbane, Australia, 23 September 2012
16. van der Wall, B.G.: Grundlagen der Hubschrauber-Aerodynamik, 1st edn. VDI-Buch. Springer Berlin Heidelberg, Berlin, Heidelberg (2015)
17. Krenik, A., Weiand, P.: Aspects on Conceptual and Preliminary Helicopter Design. Deutscher Luft- und Raumfahrtkongress 2016, Braunschweig, D, 13 - 15 September, 2016
18. Kunze, P.: Parametric Fuselage Geometry Generation and Aerodynamic Performance Prediction in Preliminary Rotorcraft Design. 39th European Rotorcraft Forum, Moscow, Russia, 3-6 September, 2013
19. Maskew, B.: Program VSAERO theory document - NASA CR-4023, Redmond, WA (1987)
20. Keys, C.N., Wiesner, R.: Guidelines for Reducing Helicopter Parasite Drag. Journal of the American Helicopter Society **20**(1), 31-40 (1975)
21. Beltramo, M.N., Morris, M.A.: Parametric study of Helicopter Aircraft Systems Costs and Weights - NASA-CR-152315, Moffett Field, CA, USA (1980)
22. Prouty, R.W.: Helicopter performance, stability, and control. Krieger, Malabar Fla. (2005)
23. Palasis, D.: Erstellung eines Vorentwurfsverfahrens für Hubschrauber mit einer Erweiterung für das Kipprotorflugzeug. Fortschrittberichte VDI(Reihe 7, Nr. 201) (1992)
24. Kaletka, J., Kurscheid, H., Butter, U.: FHS, the new research helicopter: Ready for service. Aerospace Science and Technology (2005). doi: 10.1016/j.ast.2005.02.003